

Published in final edited form as:

Hypertension. 2010 November ; 56(5): 920–925. doi:10.1161/HYPERTENSIONAHA.110.160549.

Distal Shift of Arterial Pressure Wave Reflection Sites with Aging

Jun Sugawara, Ph.D.^{1,2}, Koichiro Hayashi, Ph.D.¹, and Hirofumi Tanaka, Ph.D.²

¹Human Technology Research Institute, National Institute of Advanced Industrial Science and Technology, Ibaraki, Japan

²Cardiovascular Aging Research Laboratory, Department of Kinesiology and Health Education, University of Texas at Austin, Austin, Texas

Abstract

An early return of reflected waves, the backward propagation of the arterial pressure wave from the periphery to the heart, is associated with the augmentation of central pulse pressure and cardiovascular risks. The location of arterial pressure wave reflection, along with arterial stiffening, have a major influence on the timing of the reflected wave. To determine the influence of aging on the location of a major reflection site, arterial length (via three-dimensional artery tracing of magnetic resonance imaging) and central (carotid-femoral) and peripheral (femoral-ankle) pulse wave velocity were measured in 208 adults varying in age. The major reflection site was detected by carotid-femoral pulse wave velocity and the reflected wave transit time (via carotid arterial pressure wave analysis). The length from the aortic valve to the major reflection site (e.g., effective reflecting length) significantly increased with aging. The effective reflecting length normalized by the arterial length demonstrated that the major reflection sites located between the aortic bifurcation and femoral site in most of the subjects. The normalized effective reflecting length did not alter with aging until 65-year-old and increased remarkably thereafter in men and women. The effective reflecting length was significantly and positively associated with the difference between central and peripheral pulse wave velocity ($r=0.76$). This correlation remained significant even when the influence of aortic pulse wave velocity was partial out ($r=0.35$). These results suggest that the major reflection site shifts distally with aging partly due to the closer matching of impedance provided by central and peripheral arterial stiffness.

Keywords

arterial stiffness; arterial wave reflection; magnetic resonance image

Clinical importance of the backward propagation of the arterial pressure wave (e.g., wave reflection from the periphery to the heart) has been well recognized. In healthy young adults, the reflected wave normally returns to the central aorta in diastole and acts to maintain diastolic perfusion pressure in the coronary artery circulation^{1–3}. If the reflected wave comes back earlier to the heart (i.e., in the late systole) with aging or disease processes, however, central systolic and pulse pressure would be augmented and at the same time

Correspondence: Jun Sugawara, PhD Human Technology Research Institute National Institute of Advanced Industrial Science and Technology (AIST) Tsukuba Central 6, Tsukuba Ibaraki, 305-8566 JAPAN Tel: 81-29-861-7138 Fax: 81-29-861-6660 jun.sugawara@aist.go.jp.

Disclosures No Conflicts of interest.

This is a PDF file of an unedited manuscript that has been accepted for publication. As a service to our customers we are providing this early version of the manuscript. The manuscript will undergo copyediting, typesetting, and review of the resulting proof before it is published in its final citable form. Please note that during the production process errors may be discovered which could affect the content, and all legal disclaimers that apply to the journal pertain.

coronary perfusion pressure could be depressed. Such cardiac effects of central pressure may not be readily seen if only peripheral (brachial) pressure is assessed. For these reasons, central aortic pressure is considered to be more relevant than the standard peripheral (brachial) measure for the prediction and pathophysiology of cardiovascular disease^{4–8}. Among a number of factors determining the early return of reflected waves from the periphery to the heart (e.g., the increase in pulse wave velocity and the change in aortic diameter), the location of arterial pressure wave reflection has been shown to play an important role.

In the arterial tree, branching points (i.e., aortic bifurcation, branches of renal arteries), areas of alteration in arterial elastance (from elastic artery to muscular artery), and high-resistance arterioles can all give rise to wave reflection¹. The principal arterial wave reflection site is thought to be located at the lower abdominal aorta, more specifically at the iliac bifurcation and the renal arterial branches⁹. The traditional view is that with advancing age, aortic pulse wave velocity (PWV) increases and reflecting sites shift proximally toward the heart^{10, 11}. These changes are believed to contribute to early wave reflections seen with advancing age. However, a report from the Framingham Heart Study¹² showed that unproportionally greater increases in elastic artery PWV relative to muscular artery PWV results in impedance matching between central aorta and proximal muscular arteries, which reduces proximal wave reflection and causes distal shifts of reflecting sites. Thus, the influence of aging on the location of a reflection site remains highly controversial. The discrepancy in the literature may be due to the different methods of acquiring the inflection point of arterial waveform (e.g., the timing of the return of reflected wave) and/or a failure to account for the age-related changes in arterial length^{13, 14}. Accordingly, the experimental aim of the present study was to determine the impact of aging on the effective reflecting distance from the standing points of the possible shift of location of a major reflection site as well as the age-related ascending aortic elongation we previously reported. The aortic length was directly measured using three-dimensional imaging analysis of magnetic resonance artery images.

Methods

Subjects

A total of 208 adults (100 men and 108 women, 19–79 years) were studied. Women who were pregnant or subjects with implants that are electrically, magnetically, or mechanically active, with intracranial aneurysm clips, with cardiovascular disease, or with epileptic seizures or claustrophobic symptoms were excluded. Twenty seven subjects were taking prescribed anti-hypertensive (n=16), cholesterol lowering (n=4), diabetic (n=2), and other (e.g., thyroid hormone, anti-coagulation; n=4) medications. This study was reviewed and approved by the Institutional Review Board of the institution. All potential risks and procedures of the study were explained to the subjects, and they gave their written informed consent to participate in the study.

Experimental Protocol

All measurements were performed after 3 hour fasting and an abstinence of caffeine. Subjects were studied under supine resting conditions in a quiet, temperature-controlled room (24–26°C).

Measurements

Blood Pressure and Heart Rate—Brachial blood pressure and heart rate were measured with oscillometric pressure sensor cuffs and electrocardiograms (VP-2000, Colin Medical, San Antonio, TX). Radial artery pressure waveforms were recorded by a validated applanation tonometry-based automated radial blood pressure measurement device

(HEM-9010AI; Omron Healthcare, Kyoto, Japan) at 500 Hz of sampling rate and resampled at 128 Hz with a data acquisition and analysis software (AcqKnowledge, BIOPAC Systems, Inc., Santa Barbara, CA). Then, the arterial waveform data were fed into the SphygmoCor software (AtCor Medical, Sydney, Australia), and a generalized transfer function was applied to estimate aortic blood pressure. Radial pressure wave form was calibrated with oscillometry-derived brachial mean and diastolic blood pressure.

Pulse Wave Velocity—Aortic (carotid-femoral) and leg (femoral-ankle) PWV were measured as previously described^{13, 15}. Electrocardiogram, bilateral brachial and ankle blood pressures, carotid, femoral, and bilateral post-tibial arterial pulse waveforms were simultaneously measured with a vascular testing device (VP-2000, Colin Medical, San Antonio, TX). PWV was calculated from the distance between two arterial recording sites divided by the transit time. Carotid and femoral artery pulse waves were measured with arterial applanation tonometry incorporating an array of 15 micropiezoresistive transducers attached on the left common carotid and left common femoral arteries. Bilateral post-tibial arterial pressure waveforms were stored by cuffs connected to a plethysmographic sensor and an oscillometric pressure sensor wrapped on both ankles. The transit time between carotid and femoral ($T_{\text{car-fem}}$) and between femoral and post-tibial arterial pressure waveforms were acquired with the foot-to-foot method.

The arterial path length was computed by the three-dimensional tracing of magnetic resonance images (MRI) (via 1.0T MRI system, Magnetom Impact, Siemens, Tokyo, Japan) with image analysis software (MRIcro 1.40, Chris Roden, Columbia, SC) as previously reported¹³. The mean measurement error for this procedure was $0.3 \pm 0.2\%$. The ascending and descending aortic lengths were defined as distances from the base of the ascending aorta to the top of aortic arch and from the top of aortic arch to the level of the aortic bifurcation. The arterial path length for aortic PWV was assumed the distance from the base of the ascending aorta to the femoral recording site subtracted by the distance from the base of ascending aorta to the carotid recording site. The arterial path length for leg PWV was estimated using the validated equation ($0.249 \times \text{height [cm]} + 30.7$)¹⁵. The day-to-day coefficients of variation are $3.2 \pm 2.5\%$ and $3.7 \pm 2.2\%$ for aortic and leg PWV in our laboratory.

Carotid augmentation index—Carotid arterial pressure waveforms were recorded from common carotid artery using an applanation tonometry sensor. A neck collar device was used to secure and stabilize the applanation tonometry sensor. Carotid augmentation index (AIx) was calculated as pressure wave above its systolic shoulder (ΔP) divided by pulse pressure¹⁶. The systolic foot and shoulder of carotid arterial pressure waveforms were automatically detected by using algorithms of the measurement device based on a band-pass filtering (5–30 Hz) and fourth order derivatives, respectively¹⁵.

Effective reflecting distance—The length from the origin of left common carotid artery at aortic arch to the major reflection site (Larch-ref) was obtained from the time of return of the reflected wave (T_{ref}) and aortic PWV: $\text{Larch-ref} = (T_{\text{ref}} \times \text{aortic PWV})/2$ (Figure 1)¹². T_{ref} was obtained with the combination of the carotid arterial waveform decomposition and the cross-correlation of forward and backward waves. At first, carotid arterial pressure waveforms obtained with an arterial applanation tonometer were decomposed into forward and backward waves using a triangular flow wave method validated by Westerhof et al.¹⁷. Then, T_{ref} was determined by the cross-correlation of forward and backward waves reported by Qasem and Avolio¹⁸ with the minor modification. Briefly, cross-correlation was applied on both waves from foot to systolic peak normalized to the same amplitude. The time lag at the highest correlation between normalized forward and backward waves was defined as T_{ref} . The time of return of reflection wave was also evaluated using the time lag from the

systolic foot to the inflection point of carotid pressure (T_{ref_inf}). The inflection point was detected by the second-order derivatives. Then, the length from the origin of left common carotid artery at aortic arch to the major reflection site was obtained from T_{ref_inf} and aortic PWV ($L_{arch-ref_inf}$).

The effective reflecting distance (ERD) was taken as the length from the aortic valve to the major reflection site (e.g., the combined length of the ascending aortic length and $L_{arch-ref}$). In order to clarify the relative location of the major reflection site, the ERD was normalized by the distances from the aortic valve to the aortic bifurcation (the aortic length) and from the aortic valve to the femoral site (L_{av-fem}). Likewise, $L_{arch-ref}$ was normalized by the distance from the top of the aortic arch to the aortic bifurcation.

Statistical Analyses

Univariate and partial correlation and regression analyses were performed to determine the relations between selected physiological variables. Stepwise forward multiple-regression analysis was used to determine independent physiological correlates of aortic ERD. Two-way ANOVA was used to examine the effect of aging and sex-difference on the effective length. In the case of a significant F value, a post-hoc test using the Newman-Keuls method identified significant differences among mean values. All data are reported as mean \pm SD. Statistical significance was set *a priori* at $P<0.05$.

Results

Table 1 displays physiological and hemodynamic characteristics of subjects in four age-categories (e.g., 19–34, 35–49, 50–64, and 65–79 years old) stratified for sex. Both aortic and brachial blood pressures increased significantly with age. Brachial blood pressures were significantly higher in men than women, whereas no such differences were seen in aortic pressures.

As shown in Table 2, the aortic length was significantly longer in men than women and increased with aging. Aortic and leg PWV and carotid AIx significantly increased with aging, whereas the difference between aortic PWV and leg PWV (Δ aortic PWV-leg PWV) significantly decreased with aging. Aortic PWV was lower and carotid AIx was higher in women than in men. T_{ref} and T_{ref_inf} shortened with aging, whereas $L_{arch-ref}$ and $L_{arch-ref_inf}$ significantly increased with aging.

Figure 2 depicts the relation between the ERD normalized by the aortic length (x-axis) and L_{av-fem} (y-axis). If the latter value is larger than 1.0, the major reflection point locates distally to the femoral site. As shown in this figure, the major reflection sites existed between the aortic bifurcation and the femoral site in most subjects ($n=150$, 72%), whereas the major reflection sites located proximally to the aortic bifurcation in 45 subjects (22%) and distally to the femoral site in 13 subjects (6%).

Figure 3 represents the ERD of 4 age category groups in men and women. The ERD was longer in men than in women and increased significantly with advancing age in both sexes. The ERD remained greater in men than in women even after the normalization for the entire aortic length. These values did not change with aging until 65 years of age and increased remarkably thereafter in men and women. This change was greater in men than in women.

The ERD was correlated with Δ aortic PWV-leg PWV ($r=0.76$, $P<0.0001$). This correlation remained significant even when the influence of aortic PWV was partial out ($r=0.35$). A forward step multi-regression analysis revealed that Δ aortic PWV-leg PWV ($\beta=0.54$), the ascending aortic length ($\beta=0.31$), mean arterial pressure ($\beta=0.39$), heart rate ($\beta=-0.13$), and

sex ($\beta=0.08$) were significant independent determinant of the ERD. Furthermore, ERD ($\beta=-0.87$, $P<0.01$), as well as mean arterial pressure ($\beta=0.60$, $P<0.0001$), heart rate ($\beta=-0.32$, $P<0.0001$), aortic PWV ($\beta=1.07$, $P<0.0001$), and T_{ref} ($\beta=0.49$, $P<0.01$) were significant independent determinants of aortic pulse pressure (Table 3).

Discussion

Major findings of this study were as follows. First, a combination of arterial waveform analyses and 3-dimensional MRI indicates that the major effective arterial pressure reflection sites are located between the aortic bifurcation and femoral artery measurement site (inguinal region) in most cases (>70%). Second, the major reflection site did not change with aging until 65 years of age but shifted distally thereafter. This change was more pronounced in men than in women. Third, the effective reflecting distance (e.g., the distance from the heart to the reflection site) was significantly and positively associated with the difference between central and peripheral PWV, suggesting that the age-related distal shift of arterial wave reflection site may be attributed to the closer matching of impedance provided by central and peripheral arterial stiffness.

One unique aspect of the present study is the use of a combination of direct arterial length measurement via MRI and the detection of the major reflection site through the validated method of carotid forward- and backward pressure wave separation^{17, 18} and aortic PWV measurement¹³. Aortic (carotid-femoral) PWV values are greatly affected by the arterial path length measurement^{13, 19, 20}. For example, the use of the straight distance between carotid-femoral sites provides more than 30% higher PWV values than that obtained by the arterial path length with subtraction of the carotid length (e.g., opposite direction)²⁰. Aortic (carotid-femoral) PWV was calculated with the arterial path length directly measured with MRI in the present study. The use of the combined methodologies allowed us to determine the anatomical location of the effective reflecting distance. A study using the invasive arterial pressure recording by catheter with multiple manometers⁹ suggested that there were two major reflection sites locating at the aortic level of the renal arterial branches and distal to terminal aortic bifurcation because the pulse wave velocity and apparent phase velocity changed remarkably around these regions. However, the number of subjects was small ($n=9$). The current study involving more than 200 subjects demonstrated that the major arterial pressure reflection site is located between the aortic bifurcation and femoral site in most cases (>70%). Our findings are in general consistent with the previous invasive study using a catheter⁹.

The effective reflecting distance increased with advancing age. That is, the major reflection site shifted distally after 65 years old. These findings are consistent with the previous study by Michell et al¹². They speculated that disproportionate changes in central and peripheral arterial stiffness lead to impedance matching between central aorta and proximal muscular arteries, which might be attributed to the distal shift of reflecting sites. In order to determine the direct effect of the impedance mismatch on the age-related elongation of effective reflecting distance, we measured both aortic and leg PWV. The effective reflecting distance correlated significantly with Δ aortic PWV-leg PWV. This correlation remained significant even when the influence of aortic PWV was partial out. Furthermore, the forward stepwise multi-regression analysis revealed that Δ aortic PWV-leg PWV was a significant independent determinant of the effective reflecting distance. Together, our results are consistent with the notion that with advancing age, impedance provided by central and peripheral conduit arteries gets closer to a state of matching.

Multi-regression analyses revealed that the effective reflection distance was a significant and negative independent determinant of aortic pulse pressure even when aortic PWV and T_{ref}

were included in the model. We could interpret that the age-related elongation of effective reflecting distance, involving distal shift of the major reflection point and the structural change (e.g., tortuosity of aorta), may partly attenuate the increase in central pulse pressure with aging.

Possible limitations in the methodology should be emphasized. First, we decomposed carotid arterial pressure waveforms into forward and backward waves using a triangular flow wave method. Although this approximation may be different from the actual flow wave, this procedure has been validated¹⁷. Second, we used the cross-correlation of forward and backward waves, which may be more objective and reliable than the other methods previously used¹⁸. Importantly, although the time of return of the reflected wave (T_{ref}) may be affected by different pressure waveform analyses (i.e., derivatives)¹¹, similar results were obtained when T_{ref} was determined by the second-order derivatives. Third, we acquired aortic blood pressure noninvasively from radial arterial waveform by applying general transfer function. Although this procedure has been well-established as a reliable noninvasive measurement of central blood pressure, several issues and concerns (i.e., individualization of transfer function, calibration procedure, etc.) have been raised about this procedure^{21–23}. Lastly, Westerhof et al.²⁴ using the modeling experiments indicated that the moment of return of the reflected wave depends not only on wave speed and distance of the reflection site but also the time delay introduced by the reflection site. The time delay was assumed to be constant in the present study. However, the net effect, i.e. that the ERD increases with increasing Δ aortic PWV-leg PWV, was correctly predicted by that study.

In conclusion, the present findings demonstrated that the effective reflecting distance increases with advancing age.

Perspectives

As the early detection and prevention of vascular disease, including arterial stiffening, are widely promoted, the use of aortic (carotid-femoral) PWV has been gaining popularity as the primary modality to assess arterial stiffness. Recently, a new technique to evaluate aortic PWV using the time of the return of reflection wave via the waveform analysis from pressure waves recorded at a single site has been proposed¹⁸. However, such methodology is based on assumptions that the reflection site is fixed at the aortic or femoral bifurcation and does not move with aging. The present study findings, considered together with the previous studies^{12, 24}, indicate that this assumption may not be valid.

Acknowledgments

This study was supported in part by Special Coordination Funds of the Japanese Ministry of Education, Culture, Sports, Science, and Technology (16700499), Postdoctoral Fellowships for Research Abroad of Japan Society for the Promotion of Science, NIH award AG20966, and UT-Austin Imaging Research Center.

Funding Sources Special Coordination Funds of the Japanese Ministry of Education, Culture, Sports, Science, and Technology (16700499), Postdoctoral Fellowships for Research Abroad of Japan Society for the Promotion of Science, and NIH award AG20966.

References

1. Nichols, W.; O'Rourke, MF. McDonald's blood flow in arteries 5th ed. Theoretical, experimental and clinical principles. Arnold; London: 2005.
2. Seals DR, Stevenson ET, Jones PP, DeSouza CA, Tanaka H. Lack of age-associated elevations in 24-h systolic and pulse pressures in women who exercise regularly. *Am J Physiol* 1999;277:H947–955. [PubMed: 10484415]

3. Tanaka H, DeSouza CA, Seals DR. Absence of age-related increase in central arterial stiffness in physically active women. *Arterioscler Thromb Vasc Biol* 1998;18:127–132. [PubMed: 9445266]
4. Roman MJ, Devereux RB, Kizer JR, Lee ET, Galloway JM, Ali T, Umans JG, Howard BV. Central pressure more strongly relates to vascular disease and outcome than does brachial pressure: The strong heart study. *Hypertension* 2007;50:197–203. [PubMed: 17485598]
5. Roman MJ, Devereux RB, Kizer JR, Okin PM, Lee ET, Wang W, Umans JG, Calhoun D, Howard BV. High central pulse pressure is independently associated with adverse cardiovascular outcome the strong heart study. *J Am Coll Cardiol* 2009;54:1730–1734. [PubMed: 19850215]
6. Safar ME, Blacher J, Pannier B, Guerin AP, Marchais SJ, Guyonvarc'h PM, London GM. Central pulse pressure and mortality in end-stage renal disease. *Hypertension* 2002;39:735–738. [PubMed: 11897754]
7. Safar ME, Levy BI, Struijker-Boudier H. Current perspectives on arterial stiffness and pulse pressure in hypertension and cardiovascular diseases. *Circulation* 2003;107:2864–2869. [PubMed: 12796414]
8. Waddell TK, Dart AM, Medley TL, Cameron JD, Kingwell BA. Carotid pressure is a better predictor of coronary artery disease severity than brachial pressure. *Hypertension* 2001;38:927–931. [PubMed: 11641311]
9. Latham RD, Westerhof N, Sipkema P, Rubal BJ, Reuderink P, Murgo JP. Regional wave travel and reflections along the human aorta: A study with six simultaneous micromanometric pressures. *Circulation* 1985;72:1257–1269. [PubMed: 4064270]
10. O'Rourke MF, Nichols WW. Changes in wave reflection with advancing age in normal subjects. *Hypertension* 2004;44:e10–11. [PubMed: 15492135]
11. Segers P, Rietzschel ER, De Buyzere ML, De Bacquer D, Van Bortel LM, De Backer G, Gillebert TC, Verdonck PR. Assessment of pressure wave reflection: Getting the timing right! *Physiol Meas* 2007;28:1045–1056. [PubMed: 17827652]
12. Mitchell GF, Parise H, Benjamin EJ, Larson MG, Keyes MJ, Vita JA, Vasan RS, Levy D. Changes in arterial stiffness and wave reflection with advancing age in healthy men and women: The framingham heart study. *Hypertension* 2004;43:1239–1245. [PubMed: 15123572]
13. Sugawara J, Hayashi K, Yokoi T, Tanaka H. Age-associated elongation of the ascending aorta in adults. *J Am Coll Cardiol Img* 2008;1:739–748.
14. Wenn CM, Newman DL. Arterial tortuosity. *Australas Phys Eng Sci Med* 1990;13:67–70. [PubMed: 2375702]
15. Sugawara J, Hayashi K, Yokoi T, Cortez-Cooper MY, DeVan AE, Anton MA, Tanaka H. Brachial-ankle pulse wave velocity: An index of central arterial stiffness? *J Hum Hypertens* 2005;19:401–406. [PubMed: 15729378]
16. Kelly R, Hayward C, Avolio A, O'Rourke M. Noninvasive determination of age-related changes in the human arterial pulse. *Circulation* 1989;80:1652–1659. [PubMed: 2598428]
17. Westerhof BE, Guelen I, Westerhof N, Karmaker JM, Avolio A. Quantification of wave reflection in the human aorta from pressure alone: A proof of principle. *Hypertension* 2006;48:595–601. [PubMed: 16940207]
18. Qasem A, Avolio A. Determination of aortic pulse wave velocity from waveform decomposition of the central aortic pressure pulse. *Hypertension* 2008;51:188–195. [PubMed: 18172062]
19. Asmar, R. Arterial stiffness and pulse wave velocity: Clinical application. Elsevier; Paris: 1999.
20. Sugawara J, Hayashi K, Yokoi T, Tanaka H. Carotid-femoral pulse wave velocity: Impact of different arterial path length measurement. *Artery Research* 2010;4:27–31. [PubMed: 20396400]
21. Hope SA, Tay DB, Meredith IT, Cameron JD. Comparison of generalized and gender-specific transfer functions for the derivation of aortic waveforms. *Am J Physiol Heart Circ Physiol* 2002;283:H1150–1156. [PubMed: 12181146]
22. Mahieu D, Kips J, Rietzschel ER, De Buyzere ML, Verbeke F, Gillebert TC, De Backer GG, De Bacquer D, Verdonck P, Van Bortel LM, Segers P. Noninvasive assessment of central and peripheral arterial pressure (waveforms): Implications of calibration methods. *J Hypertens* 2010;28:300–305. [PubMed: 19901847]
23. Segers P, Carlier S, Pasquet A, Rabben SI, Hellevik LR, Remme E, De Backer T, De Sutter J, Thomas JD, Verdonck P. Individualizing the aorto-radial pressure transfer function: Feasibility of

- a model-based approach. *Am J Physiol Heart Circ Physiol* 2000;279:H542–H549. [PubMed: 10924052]
24. Westerhof BE, van den Wijngaard JP, Murgu JP, Westerhof N. Location of a reflection site is elusive: Consequences for the calculation of aortic pulse wave velocity. *Hypertension* 2008;52:478–483. [PubMed: 18695144]

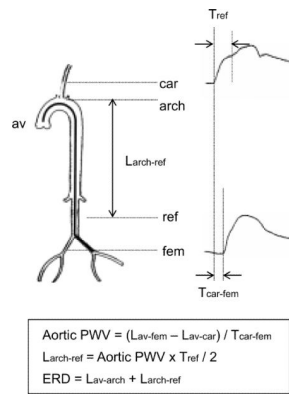


Figure 1.

Detection of effective reflection site. T_{ref} : the time delay between the systolic foot and the first inflection point of carotid arterial pressure waveform, which corresponds to the double reflected wave transit time; $T_{car-fem}$: the time delay between carotid and femoral artery pressure wave forms; L_{av-fem} : the arterial length from the aortic valve to the femoral site; L_{av-car} : the arterial length from the aortic valve to the carotid site; $L_{arch-ref}$: the arterial length from the top of aortic arch to the effective reflection site. $L_{av-arch}$: the arterial length from aortic valve to the top of aortic arch (e.g., the ascending aorta). The effective reflecting distance (ERD) is the combined length of the ascending aortic length and $L_{arch-ref}$.

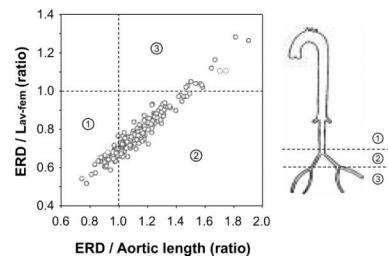


Figure 2.

The anatomical location of the major reflection site classified by the relation between the effective reflecting distances (ERD) normalized by the distance from the aortic valve to the aortic bifurcation (aortic length) and the distance from the aortic valve to femoral site (L_{av-fem}). The ERD/aortic length ratio higher than 1.0 means that the major reflection point locates at the aortic bifurcation. The ERD/ L_{av-fem} ratio higher than 1.0 means that the major reflection point locates around the femoral bifurcation.

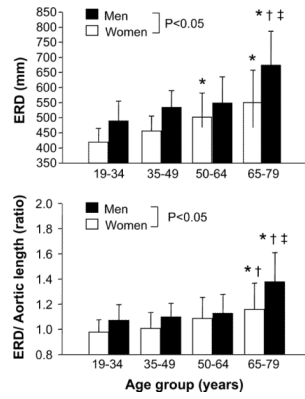


Figure 3.

Aging-related changes in effective reflecting distance (ERD). Open bars show women and closed bars show men. Data are mean and SD. Bottom panel depicts the ERD normalized by the aortic length. Open bars shows women and closed bar shows men. * $P < 0.05$ vs. “19–34” of same sex; † $P < 0.05$ vs. “35–49” of same sex; ‡ $P < 0.05$ vs. “50–64” of same sex.

Table 1

Selected Physiological Characteristics and Hemodynamics

Variables	Age category				ANOVA results		
	19-34	35-49	50-64	65-79	Sex	Age	Interaction
Number	Men 23	26	38	24			
	Women 17	19	46	26			
Age, years	Men 27 ± 5	43 ± 5	60 ± 3	70 ± 4	ns	P<0.0001	ns
	Women 28 ± 5	43 ± 5	59 ± 4	68 ± 2			
Height, cm	Men 172 ± 5	172 ± 5	167 ± 6	165 ± 7	P<0.0001	P<0.0001	ns
	Women 159 ± 6	159 ± 5	155 ± 5	152 ± 7			
Body mass, kg	Men 70 ± 12	70 ± 10	65 ± 9	62 ± 9	P<0.0001	P<0.05	ns
	Women 52 ± 5	57 ± 8	54 ± 6	52 ± 8			
Body mass index, kg/m ²	Men 23.7 ± 3.8	23.8 ± 2.9	23.4 ± 2.7	22.8 ± 2.3	P<0.0001	ns	ns
	Women 20.7 ± 1.9	22.4 ± 2.9	22.5 ± 2.4	22.5 ± 2.4			
Heart rate, bpm	Men 57 ± 10	57 ± 8	59 ± 7	58 ± 6	P<0.01	ns	ns
	Women 59 ± 9	63 ± 7	62 ± 8	62 ± 7			
Brachial SBP, mmHg	Men 117 ± 12	127 ± 19	127 ± 17	132 ± 15	P<0.01	P<0.0001	ns
	Women 104 ± 7	115 ± 13	126 ± 15	128 ± 15			
Brachial MAP, mmHg	Men 86 ± 10	98 ± 16	98 ± 13	102 ± 13	P<0.0001	P<0.0001	ns
	Women 77 ± 5	88 ± 12	96 ± 12	97 ± 13			
Brachial DBP, mmHg	Men 68 ± 9	80 ± 13	81 ± 10	81 ± 10	P<0.01	P<0.0001	ns
	Women 61 ± 5	72 ± 10	76 ± 9	77 ± 9			
Brachial PP, mmHg	Men 50 ± 6	47 ± 7	46 ± 10	51 ± 10	ns	P<0.05	P<0.05
	Women 43 ± 6	43 ± 6	50 ± 9	51 ± 10			
Aortic SBP, mmHg	Men 106 ± 14	118 ± 22	119 ± 20	129 ± 19	P<0.0001	P<0.0001	ns
	Women 94 ± 9	105 ± 15	120 ± 18	121 ± 19			
Aortic PP, mmHg	Men 37 ± 10	37 ± 10	37 ± 13	47 ± 15	ns	P<0.0001	P<0.05
	Women 32 ± 10	31 ± 8	43 ± 13	43 ± 15			
Brachial PP/aortic PP ratio	Men 1.83 ± 0.36	1.43 ± 1.28	1.19 ± 0.16	1.14 ± 0.10	P<0.0001	P<0.0001	P<0.01
	Women 1.49 ± 0.26	1.20 ± 0.16	1.10 ± 1.10	1.09 ± 0.14			

Data are mean±SD. SBP=systolic blood pressure, DBP=diastolic blood pressure, MAP=mean arterial pressure, PP=pulse pressure.

Table 2

Selected Arterial Properties

Variables		Age category				ANOVA results		
		19-34	35-49	50-64	65-79	Sex	Age	Interaction
Aortic PWV, cm/sec	Men	669 ± 109	829 ± 161	900 ± 164	1128 ± 214	P<0.01	P<0.0001	ns
	Women	610 ± 76	757 ± 121	870 ± 142	962 ± 169			
Leg PWV, cm/sec	Men	945 ± 89	1002 ± 97	1065 ± 155	1149 ± 107	ns	P<0.0001	ns
	Women	931 ± 89	966 ± 91	1078 ± 109	1118 ± 94			
Aortic PWV-leg PWV, cm/sec	Men	-276 ± 134	-173 ± 111	-165 ± 169	-21 ± 244	P<0.05	P<0.0001	ns
	Women	-321 ± 123	-209 ± 89	-209 ± 157	-156 ± 189			
Carotid Aix, %	Men	-12 ± 12	5 ± 15	22 ± 11	24 ± 14	P<0.0001	P<0.0001	ns
	Women	1 ± 14	15 ± 12	31 ± 8	32 ± 8			
T _{car-fem} , sec	Men	75 ± 10	64 ± 10	56 ± 7	46 ± 8	P<0.01	P<0.0001	ns
	Women	78 ± 8	67 ± 9	57 ± 8	53 ± 8			
T _{ref} , sec	Men	132 ± 13	114 ± 10	104 ± 10	104 ± 8	P<0.0001	P<0.0001	ns
	Women	124 ± 13	107 ± 8	99 ± 8	97 ± 11			
T _{ref_inf} , sec	Men	187 ± 17	163 ± 27	144 ± 24	146 ± 22	P<0.0001	P<0.0001	ns
	Women	177 ± 17	146 ± 19	128 ± 26	123 ± 23			
L _{aorta} , mm	Men	456 ± 25	486 ± 23	486 ± 27	489 ± 28	P<0.0001	P<0.0001	ns
	Women	428 ± 23	454 ± 29	461 ± 26	473 ± 29			
L _{arch-ref} , mm	Men	438 ± 64	466 ± 51	466 ± 81	584 ± 109	P<0.0001	P<0.0001	P<0.05
	Women	377 ± 46	401 ± 45	432 ± 74	469 ± 96			
L _{arch-ref_inf} , mm	Men	623 ± 95	665 ± 96	648 ± 459	819 ± 172	P<0.0001	P<0.0001	P<0.05
	Women	537 ± 62	544 ± 50	558 ± 146	599 ± 183			

Data are mean±SD. T_{car-fem}=time delay of carotid and femoral arterial pressure waveform, T_{ref}=time of return of reflected wave evaluated with the cross-correlation method, T_{ref_inf}=time of return of reflected wave evaluated with the second-order derivative method, PWV=pulse wave velocity, Aix=augmentation index, L_{aorta}=the aortic length, L_{arch-ref}=the length from the top of the aortic arch to the major reflection site estimated with T_{ref}, L_{arch-ref_inf}= the length from the top of the aortic arch to the major reflection site estimated with T_{ref_inf}.

Table 3

Summary of Forward Stepwise Regression Analyses.

Dependent Variable: Effective Reflecting Distance

Independent Variable	β	P-level	Accumulative R²
Δ aortic PWV-leg PWV, cm/sec	0.54	<0.0001	0.57
Ascending aortic length, mm	0.31	<0.0001	0.72
MAP, mmHg	0.39	<0.0001	0.76
Heart rate, beat/min	-0.13	<0.0001	0.78
Sex, female=0	0.08	<0.05	0.79

Dependent Variable: Aortic Pulse Pressure

Independent Variable	β	P-level	Accumulative R²
MAP, mmHg	0.60	<0.0001	0.42
Heart rate, beat/min	-.32	<0.0001	.48
Aortic PWV, cm/sec	1.07	<0.0001	0.49
ERD, mm	-0.87	<0.01	0.49
T _{ref} , sec	0.49	<0.01	0.51

PWV=pulse wave velocity, MAP=mean arterial pressure, T_{ref}=time of return of reflected wave evaluated with the cross-correlation method, ERD=effective reflecting distance.